Cell Tissue Res (1996) 283:493–505

Cell & Tissue Research

Analysis of projections from the cochlear nucleus to the lateral paragigantocellular reticular nucleus in the rat

Breno Bellintani-Guardia, Michaela Schweizer, Horst Herbert

Tierphysiologie, Universität Tübingen, Auf der Morgenstelle 28, D-72076 Tübingen, Germany

Received: 19 July, 1995 / Accepted: 28 November 1995

Abstract. Golgi-staining, retrograde and anterograde tract-tracing, and a two-color immunoperoxidase technique have been employed, at the light- and electron-microscopic levels, to analyze the auditory projections from the cochlear nucleus (CN) to the lateral paragigantocellular reticular nucleus (LPGi) in the rat. We have found that the auditory input originates predominantly in the posteroventral and cochlear root nuclei. The auditory axons terminate in the cell-poor, ventral portion of the LPGi, which is strongly invaded by beaded dendritic profiles, originating from parent cell bodies located in the dorsal half of the LPGi. Ultrastructural analysis has revealed that the anterogradely labeled auditory axons form functional synapses preferentially with dendritic shafts. These axo-dendritic contacts are apparently excitatory in nature. By means of a sequential two-color immunoperoxidase staining method, we have further characterized potential postsynaptic neurons in the LPGi. Black-stained auditory fibers intermingle with brown-stained serotonergic or adrenergic neurons. Varicose auditory axons are often closely apposed to immunoreactive dendritic profiles of serotonergic and adrenergic neurons, indicating the presence of possible synaptic contacts of auditory terminal fibers with these transmitter-classified cells. The monosynaptic auditory input from the CN may modulate the activity of B3 serotonergic and C1 adrenergic cells in the LPGi and may thus induce adaptive changes in response to acoustic stimuli.

Key words: Auditory system – Autonomic system – Sensomotor system – Reticular formation – Serotonin – Adrenaline – Rat (Sprague Dawley)

This study was supported by the Deutsche Forschungsgemeinschaft (HE 1842/3-1 and 3-2).

Correspondence to: H. Herbert

Introduction

In a series of studies from our laboratory, we have shown that auditory brainstem nuclei project to various reticular nuclei that lie in the rat pontine and medullary brainstem but that are not considered as part of the classical auditory pathway (Kandler and Herbert 1991; Caicedo and Herbert 1993; Klepper and Herbert 1993; Lingenhöhl and Friauf 1992, 1994; Bellintani-Guardia et al. 1994). In the reticular formation, the auditory input might be integrated with various other afferents to induce or modulate behavioral responses, such as the well-studied audio-motor reflexes of the caudal pontine reticular nucleus (e.g., Lingenhöhl and Friauf 1992, 1994). Previous reports have also demonstrated auditory projections to the lateral paragigantocellular reticular nucleus (LPGi), both in rat and in cat. The auditory fibers originate primarily in the cochlear nucleus (CN) and, to a lesser extent, in the inferior colliculus (Errington and Dashwood 1979; Andrezik et al. 1981a, b; Kamiya et al. 1988; Kandler and Herbert 1991; Caicedo and Herbert 1993; Van Bockstaele et al. 1989, 1993). Those parts of the LPGi that receive auditory afferents and that correspond in location to the "juxtafacial" portion of the LPGi (see Van Bockstaele et al. 1993) are also heavily invaded by somatosensory afferents, especially from the dorsal column nuclei (Andrezik et al. 1981b; Kamiya et al. 1988; Van Bockstaele et al. 1993). In addition to these sensory afferents, the LPGi receives projections from various other brain areas implicated in a variety of functions (summarized in Van Bockstaele et al. 1993). The efferent projections of the LPGi are widespread. They include pontine, medullary, and spinal projections to sensory, autonomic, and respiratory nuclei (Loewy et al. 1981; Strack et al. 1989; Haxhiu et al. 1993; Zagon and Smith 1993; Dobbins and Feldman 1994), and projections to the locus coeruleus (Guyenet and Young 1987, 1992; Aston-Jones et al. 1986) and to the limbic forebrain (Loewy et al. 1981; Zagon et al. 1994). The above cited studies have provided a comprehensive, but general, picture of the afferent and efferent connections

of the juxtafacial portion of the LPGi. These anatomical findings have led to the suggestion that the LPGi is a crucial integrator of polymodal sensory inputs and that it plays a role in the modulation of behavioral, sensory, and/or autonomic functions (for a review, see Van Bockstaele et al. 1993).

In order to shed more light on the potential functional significance of the auditory input to this reticular nucleus, we have analyzed primary auditory afferents from the CN to the LPGi with retrograde and anterograde tracing techniques. Furthermore, we have characterized potential postsynaptic targets of auditory axons in the LPGi. A two-color immunoperoxidase staining technique has been employed to demonstrate the co-distribution of presumed terminal axons with chemically distinct neurons. Finally, we have studied the synaptic organization of the auditory terminals in the LPGi at the electron-microscopic level. A preliminary report of this study has been published elsewhere (Bellintani-Guardia et al. 1994).

Materials and methods

Golgi staining

To characterize the morphology and dendritic arborization of neurons in the LPGi, the medullary brainstems of three rats were silver-impregnated following a rapid Golgi-staining protocol. Animals were deeply anesthetized with ether and decapitated. The brains were then quickly removed, cut into blocks of 3–5 mm thickness, and incubated in a freshly prepared solution of distilled water containing 5% potassium dicromate, 5% chloral hydrate, 1.25% paraformaldehyde, 2.5% glutaraldehyde, and 0.35% dimethyl sulfoxide. Tissue blocks were transferred daily into a freshly prepared solution. After 4 days, the blocks were incubated in silver nitrate (0.75%) for 48 h, thereafter rinsed in alcohol (50%), and cut at 100 μm in the coronal plane with a Vibratome. The sections were then dehydrated in graded alcohols, cleared in xylene, and coverslipped with Entellan. The LPGi was analyzed for Golgi-stained neurons with the light microscope and individual neurons were drawn with the aid of a camera lucida at high power (500×).

Tracing experiments

General surgical procedures. Experiments were performed on 59 female Sprague-Dawley rats weighing 200–300 g. They were anesthetized with intraperitoneal (i.p.) injections of 7% chloral hydrate (40 mg/100 g body weight) and placed in a stereotaxic device (David Kopf, Tujunga, Calif., USA) for surgical procedures. For tracer injections into the CN, the skull was exposed and a hole was drilled in the parietal bone. The positions of the injections were determined by using stereotaxic coordinates taken from the atlas of Paxinos and Watson (1986).

Retrograde tracing experiments. In order to localize auditory neurons projecting to the LPGi, 21 rats received iontophoretic injections of 2% Fluoro-Gold (FG; Fluorochrome, Englewood, Colo; USA) in 0.1 M cacodylate buffer, pH 7.5, via glass micropipettes of 30-μm to 50-μm tip diameter (+5 μA, 7 s on/off for 5–20 min). After 5–15 days, the rats were reanesthetized with an overdose of chloral hydrate (60 mg/100 g body weight, i.p.) and perfused transcardially with 25 ml 0.01 M phosphate buffer, pH 7.4, containing 0.9% NaCl (phosphate-buffered saline, PBS), followed by 500 ml ice-cold 4% paraformaldehyde (PFA) in 0.1 M phosphate buffer, pH 7.4. The brains were then removed and postfixed overnight at 4° C in this fixative plus 5% sucrose; they were transferred into 0.1 M PBS with 30% sucrose and immersed for 12 h. Frozen sections of 40–50 μm were cut in the coronal plane and divided into two series. One series was stained for Nissl-substance with thionine. The other was mounted on gelatine-coated slides, air-dried, dehydrated in graded alcohols, cleared in xylene, coverslipped with Entellan, and used for fluorescence microscopy. Sections were viewed with a microscope equipped for fluorescence illumination and a UV-filter system for FG. The distribution of retrogradely labeled neurons in the CN was plotted with a computerized plotter system coupled to the microscope stage (MDPlot; Minnesota Datametrics, St. Paul, Minn., USA). Cytoarchitectural boundaries were defined by superimposing the adjacent thionine-stained sections with the plots.

Anterograde tracing experiments. By using the anterograde tracer *Phaseolus vulgaris*-leucoagglutinin (PHA-L; Vector Laboratories, Burlingame, Calif., USA), we analyzed the distribution of auditory CN fibers in the LPGi (n=33). In most of these cases, three injections were made at slightly different rostrocaudal levels in order to increase the number of labeled fibers in the LPGi. Only sections through the medullary brainstem, which included the CN and the LPGi, were cut and analyzed. PHA-L (2.5% in 10 mM PBS, pH 8) was delivered iontophoretically via glass micropipettes with 30-μm to 60-μm tip diameters by means of a pulsed positive current (5–10 μA, 7 s on/off), which was applied for 15–30 min. After a survival time of 5–10 days, the animals were reanesthetized with an overdose of chloral hydrate (60 mg/100 g body weight, i.p.) and perfused transcardially with PBS. Fixation was started with 200 ml ice-cold 4% PFA in 0.1 M sodium acetate buffer, pH 6.5, and continued with 300 ml ice-cold 4% PFA in 0.1 M borate buffer, pH 11. The brains were removed and postfixed overnight at 4° C in the borate-buffer fixative with 5% sucrose; they were then transferred into PBS containing 30% sucrose and immersed for 12 h. Brain blocks were cut coronally on a freezing microtome at 40–50 μm. One series of sections was mounted on gelatine-coated slides, stained for Nissl substance with thionine and coverslipped. Another series was immunohistochemically processed by the peroxidase-antiperoxidase (PAP) method to identify PHA-L-labeled fibers. Sections were rinsed in several changes of TRIS-buffered saline (TBS, 50 mM, pH 7.6) and incubated in a blocking solution containing 10% normal swine serum, 2% bovine serum albumin (BSA), and 0.3% Triton X-100 in TBS. After 1 h, the sections were transferred directly into the primary antibody solution of rabbit anti-PHA-L (Dako, Hamburg, Germany), diluted 1:3000 in a carrier containing 1% normal swine serum, 1% BSA, and 0.3% Triton X-100 in TBS. The incubation in the primary antiserum was for 48 h at 4° C. The sections were then rinsed in several changes of TBS, transferred to an unlabeled swine anti-rabbit IgG antiserum (Dako), diluted 1:50 in the carrier, and incubated at room temperature for 1.5 h. They were then extensively rinsed in TBS and incubated in a rabbit-PAP complex (Dako), diluted 1:150 in the carrier, again for 1.5 h at room temperature, followed by several rinses in TBS. The final visualization of the anterogradely transported PHA-L was accomplished by processing the sections in TBS, containing 0.05% 3,3-diaminobenzidine (DAB) and 0.01% hydrogen peroxidase (H_2O_2), for 10–30 min. The incubation was stopped by transferring the sections into TBS with repeated rinsing. Finally, they were mounted on gelatine-coated slides, air-dried, dehydrated in alcohol, cleared in xylene, and coverslipped with Entellan. The sections were viewed and analyzed with a light microscope. Injection sites and anterogradely labeled fibers were drawn with a drawing tube. Cytoarchitectural boundaries were defined by superimposing the adjacent thionine-stained section on the camera-lucida drawings.

Two-color immunoperoxidase staining

Co-distribution studies. In order to demonstrate the co-distribution of PHA-L labeled fibers and structures containing serotonin (5-

HT) or phenylethanolamine N-methyltransferase (PNMT) in the LPGi, sequential PAP-staining for PHA-L and 5-HT or PHA-L and PNMT was performed (Herbert 1992). To demonstrate PHA-L-immunoreactivity, the first incubation was performed as described above. The final visualization, however, was accomplished by processing the sections with nickel-enhanced DAB (Ni-DAB), i.e., 0.6% nickel-ammonium sulfate, 0.02% DAB, and 0.01% H_2O_2 in TBS. The PHA-L-immunoreactive (ir) fibers visualized with Ni-DAB appeared black. In the second incubation, the same series of sections were processed to demonstrate serotonergic and adrenergic structures in the tissue. They were rinsed in TBS and incubated in the blocking solution. After 1 h, the sections were transferred into the primary antibody solutions, viz., either rabbit anti-5-HT (1:2000; Eugene Tech, Allendale, NJ., USA) or rabbit anti-PNMT (1:2500; Incstar, Stillwater, Minn; USA), and incubated for 48 h at 4 ° C. The remaining steps were the same as described previously. The 5-HT-ir and PNMT-ir structures visualized with the standart DAB reaction appeared light brown.

Controls. As all primary antisera used were raised in rabbits, the specificity of the immunohistochemical staining was assured by controls. Omission of either one of the primary antisera in the two-color immunoperoxidase protocol always resulted in the specific labeling of one antigen only. Moreover, sections that were stained for the PHA-L alone always exhibited the same fiber patterns as adjacent sections that were taken from the same brain and that were processed following the double-staining protocol. The Ni-DAB reaction was always carried out first, thereby avoiding blackening of formerly brown reaction product. Furthermore, the morphological differences between axons and dendritic processes were clearly distinguishable, so that false-positive labeling caused by cross-reactivity would easily have been detected by light microscopy. Finally, it was assumed that the DAB-polymerization product masked the immunocomplex and, thus, prevented binding of the antisera applied in the second incubation step to the first immunocomplex (Joseph and Piekut 1986).

Data analysis. Sections were analyzed by light microscopy using a 100× oil-immersion objective. Photomicrographs were taken of PHA-L labeled varicosities in contact with 5-HT-ir or PNMT-ir somata or processes. This was performed when both were in the same plane of focus, when beaded fibers tracked the shape of somatic or dendritic profiles, or when axons exhibited varicosities exactly at the point where they crossed 5-HT-ir or PNMT-ir somata or processes. These points of close association were regarded as presumed synaptic contacts between auditory fibers and 5-HT-ir or PNMT-ir neurons in the LPGi.

Electron microscopy

With the aim of investigating the ultrastructural morphology of CN fibers in the LPGi, the immunohistochemical demonstration of PHA-L labeled auditory fibers was combined with electron-microscopic techniques. Two rats received PHA-L injections as described above. After 5–10 days of survival, they were deeply anesthetized with an overdose of chloral hydrate (60 mg/100 g body weight, i.p.) and transcardially perfused with 200 ml 0.1 M PBS followed by 250 ml ice-cold 4% PFA in 0.1 M PBS, pH 7.4, containing 15% picric acid. The brains were then removed and postfixed overnight in the PFA-picric acid fixative at 4° C. Vibratome sections (50 µm thick) were cut from the brain stem in the coronal plane and incubated in a series of ethanols (10%, 20%, 40%, 20%, 10%) for 10 min each (Eldred et al. 1983). This procedure improved antibody penetration without distroying membranes. PHA-L immunohistochemistry was carried out as described above, except that Triton X-100 was omitted in all incubation steps. After the DAB reaction, the sections were postfixed with 2% glutaraldehyde in PBS for 30 min, followed by an incubation in 1% osmium tetroxide in 0.1 M PBS for 30 min on ice. After several washes in PBS, the sections were dehydrated and mounted on slides with Epon resin between acetate foils and cured for 48 h at 60° C. Regions of the LPGi containing PHA-L-labeled terminals were selected under the light microscope and mounted on Epon blocks. Ultrathin sections (60 nm) were cut with a Reichert-Jung ultramicrotome (Leica, Stuttgart, Germany), collected on pioloform-coated slot grids, counterstained with 2.5% uranyl acetate and lead citrate, and examined with a Zeiss 902 electron microscope (Zeiss, Oberkochen, Germany). Labeled profiles in the LPGi were photographed at 12000× or 20000× magnification and examined for synaptic contacts.

Results

Anatomical location and cytoarchitecture of the LPGi

The LPGi, as referred to in the present study, is located in the ventromedial medulla, bordering the facial nucleus laterally and the gigantocellular reticular nucleus and the pyramidal tract medially (Fig. 1). Rostrally, the LPGi extends to the posterior aspects of the superior olivary complex, whereas the caudal boundary is formed by the rostroventrolateral reticular nucleus and the inferior olive. In Nissl-stained sections, the LPGi exhibits a typical reticular appearance with small to medium-sized neurons embedded in the spaces formed by rostroventrally

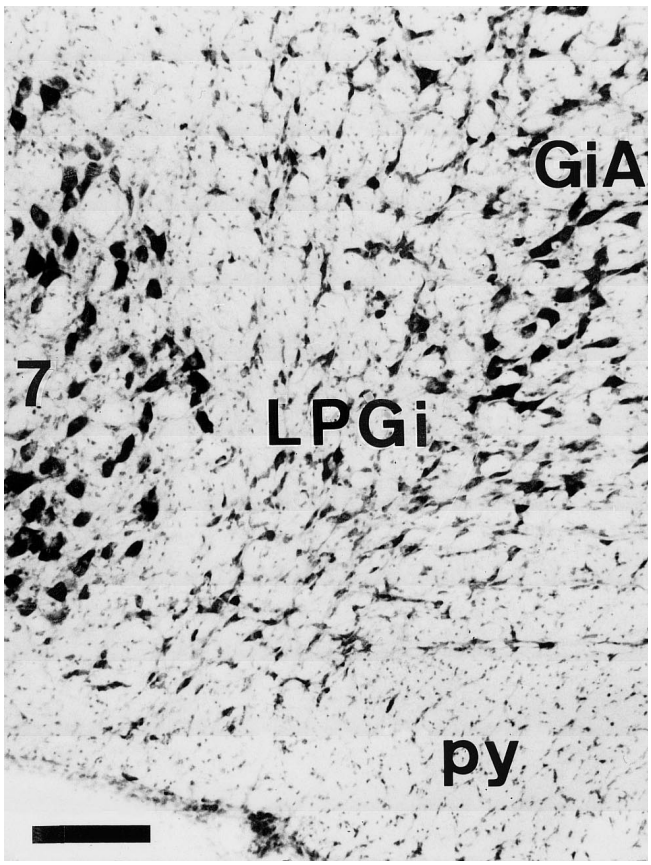

Fig. 1. Photomicrograph of a thionine-stained coronal section through the rat brainstem, illustrating the location of the lateral paragigantocellular nucleus (*LPGi*) in the ventromedial medulla. The LPGi, as defined in the present study, is bordered by the facial nucleus laterally (*7*), and by the pyramidal tract (*py*) and the gigantocellular reticular nucleus, pars alpha (*GiA*) medially. *Bar*: 250 µm

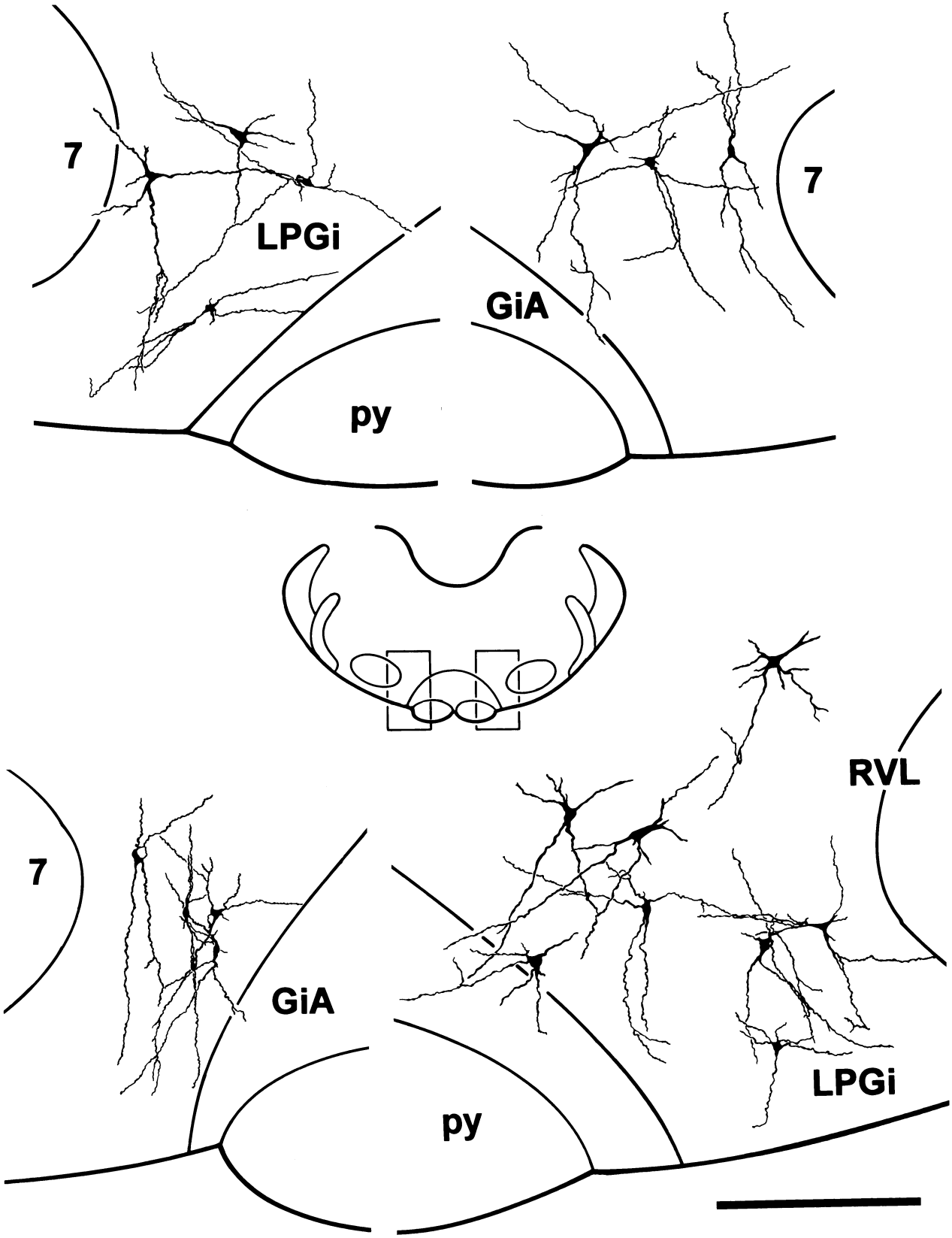

Fig. 2. Camera lucida drawings of Golgi-stained neurons in the LPGi to illustrate their dendritic morphology. *Inset* (center) depicts the relative locations of the areas shown in the *upper* and *lower left* and *right panels*. Note that many neurons exhibit dorsoventrally running dendrites that invade even the most ventral aspects of the LPGi. *7* Facial nucleus; *GiA* gigantocellular reticular nucleus, alpha; *py* pyramidal tract; *RVL* rostroventrolateral reticular nucleus. *Bar:* 500 μm

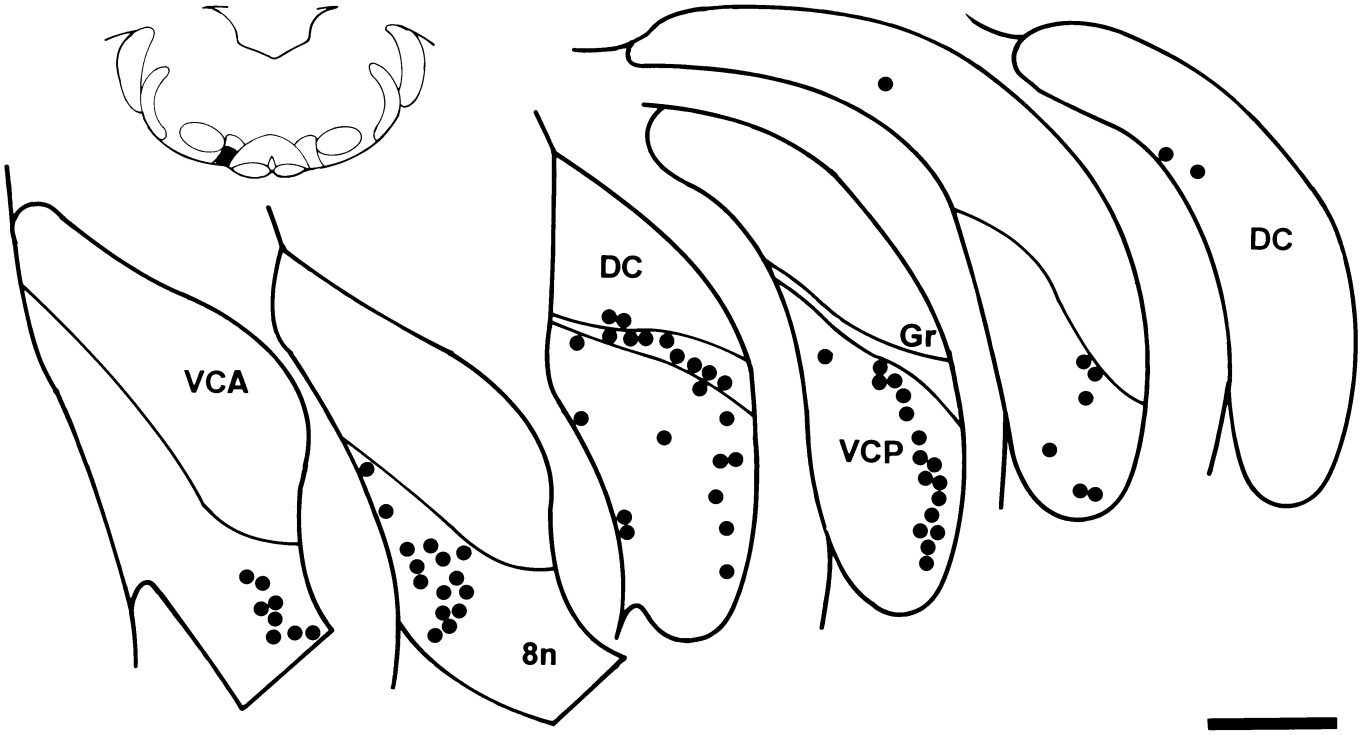

Fig. 3. Series of coronal sections through the CN (*left to right*, from rostral to caudal), demonstrating the distribution of retrogradely labeled neurons after an FG injection into the LPGi. The injection site is depicted by the *dark shading* in the *inset*. Note that labeled neurons are predominantly present in the posteroventral CN (*VCP*) and in the cochlear root nucleus located within the acoustic nerve (*8n*). *DC* Dorsal cochlear nucleus; *Gr* granular layer cochlear nucleus; *VCA* anteroventral cochlear nucleus. *Bar:* 500 μm

running fascicles. The distribution of somata within the LPGi is not uniform in terms of packing density. The most ventral portion appears as a cell-poor region compared with the dorsal part of the LPGi.

In order to collect further information on the neuropil comprising the LPGi, we analyzed Golgi-stained sections. The parent cell bodies of the majority of Golgi-stained neurons were located in the dorsal portion of the LPGi (Fig. 2), with only a few Golgi-stained neurons beeing seen in the ventral LPGi (Fig. 2, upper left and lower right). This finding was expected and in agreement with the observations in Nissl-stained material. We most frequently observed that the dorsally located cell bodies gave off dorsoventrally running dendrites that markedly invaded the cell-poor region of the ventral LPGi (Fig. 2). These dendrites usually had a beaded appearance indicative of sites of synaptic contacts. In our material, LPGi neurons with ventrally travelling dendrites were the predominant cell type. The few Golgi-stained neurons observed in the ventral LPGi often had mediolaterally oriented dendritic trees (e.g., Fig. 2, upper left).

Retrograde tracing experiments

We injected the retrograde fluorescent tracer FG into various rostrocaudal or dorsoventral levels of the LPGi of 21 rats and mapped the distribution of retrogradely labeled neurons in auditory brainstem nuclei. In the present study, we concentrated on labeled neurons in the CN, these neurons probably being exclusively involved in the transmission of auditory information. FG injections into the ventral aspects of the LGPi at various rostrocaudal levels along the facial nucleus (n=11) resulted consistently in retrogradely labeled neurons in the CN. The majority of labeled neurons was found in the posteroventral CN (Fig. 3). Interestingly, in some cases, we observed bands of labeled neurons running along the whole dorsoventral extent of the posteroventral CN (Fig. 3, middle sections), thereby crossing the isofrequency laminae perpendicularly. Many labeled neurons were also present in the cochlear root nucleus, the neurons of which were embedded within the fascicles of the auditory nerve (Fig. 3, left sections, 8n). Labeled neurons were only occasionally found in the remaining nuclei of the CN.

Control injections centered dorsally to the LPGi in the reticular formation or laterally within the gigantocellular reticular nucleus led to only scattered labeling or no labeling at all in the CN. In contrast, FG injections that were placed too far rostrally and that probably involved the caudal part of the superior olivary complex, i.e., the caudal periolivary region, resulted in strong labeling in various auditory nuclei. These cases were excluded from our pool of data but served as valuable controls in establishing the specificity of the remaining experiments.

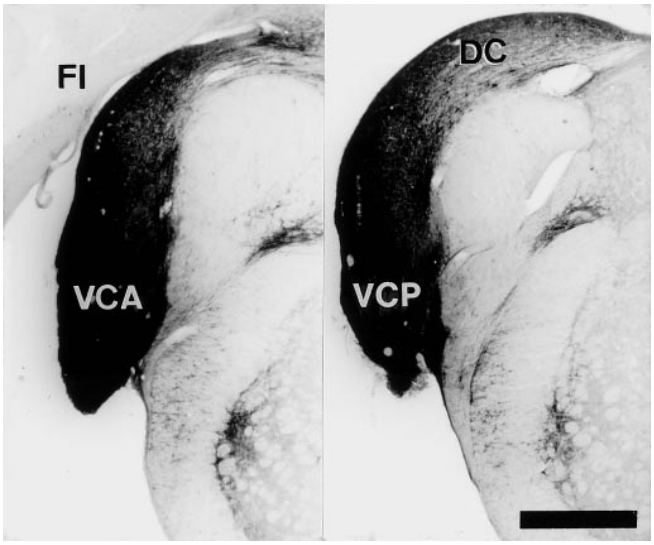

Fig. 4. Coronal sections through the CN of one animal (*left to right*, from rostral to caudal) showing a large PHA-L injection site including the anteroventral (*VCA*) and the posteroventral (*VCP*) nuclei. Note that the tracer is clearly restricted to the CN without any spread into adjacent structures. *DC* Dorsal cochlear nucleus; *FL* flocculus. *Bar:* 500 μm

Anterograde tracing and immunohistochemistry for 5-HT and PNMT

In order to analyze the distribution of auditory fibers in the LPGi, we injected the anterogradely transported tracer PHA-L into the CN. PHA-L injections centered on the posteroventral CN (Fig. 4) were most effective in labeling large numbers of auditory terminals in the LPGi, whereas injections into the dorsal or anteroventral CN led only to scattered labeling of fibers. This was in agreement with our findings from the retrograde tracing experiments. In those cases where the posteroventral CN was injected (n=12), labeled fibers were most numerous and extended from the rostral portion of the LPGi (Fig. 5A) along the complete rostrocaudal length of the facial nucleus (Figs. 5B, C, 7A, B). Caudally to the facial nucleus, the labeling faded out, reaching only slightly into the anterior pole of the rostroventrolateral reticular nucleus (Figs. 5D, 7C). We consistently observed terminal CN-fibers predominantly in the ventral cell-poor region of the LPGi (Figs. 5, 7).

One aim of the present study was to identify, in the LPGi, neurons that are potential targets of efferent fibers from the CN. Therefore, sections that had previously been processed for PHA-L immunoreactivity using Ni-DAB as the chromogen were subsequently stained for their immunoreactivity for 5-HT or PNMT and thereafter analyzed by light microscopy. With regard to 5-HT-ir structures, a considerable degree of overlap between auditory axons in the LPGi and most laterally located 5-HT-ir neurons and dendritic processes of the B3 serotonergic cell group was observed (Fig. 5). In these sections, black-stained beaded fibers were frequently seen closely apposed to brown-stained 5-HT-ir elements. Presumed terminal and *en passant* varicosities were predominantly found in close apposition to 5-HT-ir proximal dendrites (Fig. 6A–D) and to 5-HT-ir processes that

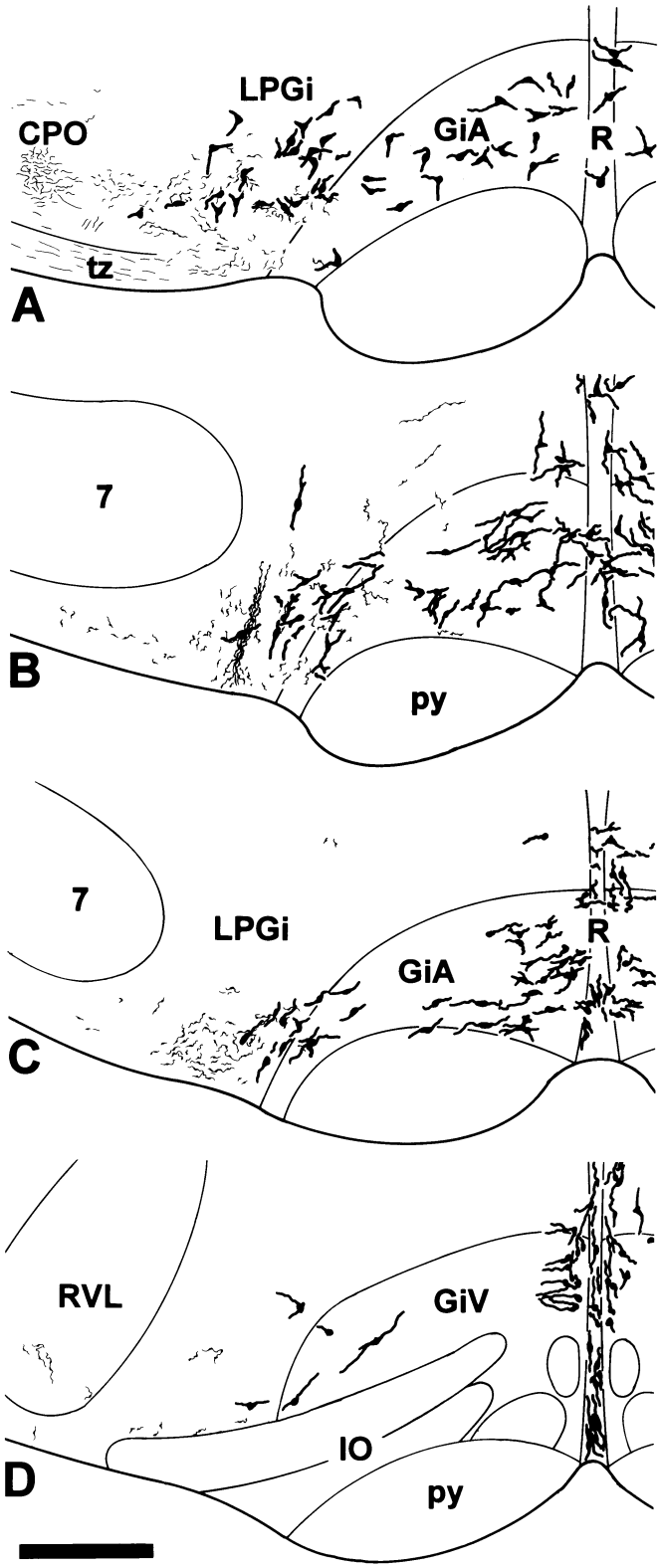

Fig. 5A–D. Camera lucida drawings of coronal sections through the medullary brainstem, from rostral to caudal, illustrating the co-distribution of anterogradely labeled auditory fibers from the CN (depicted by *thin curved lines*) and 5-HT-ir neurons of the B3 serotonergic cell group (depicted by *thick lines*) in the LPGi. Note that the majority of labeled fibers is present in the ventral aspect of the LPGi (**B, C**). *7* Facial nucleus; *CPO* caudal periolivary nucleus; *GiA* gigantocellular reticular nucleus, alpha; *GiV* gigantocellular reticular nucleus, ventral; *IO* inferior olive; *py* pyramidal tract; *R* raphe nucleus; *RVL* rostroventrolateral reticular nucleus; *tz* trapezoid body. *Bar:* 500 μm

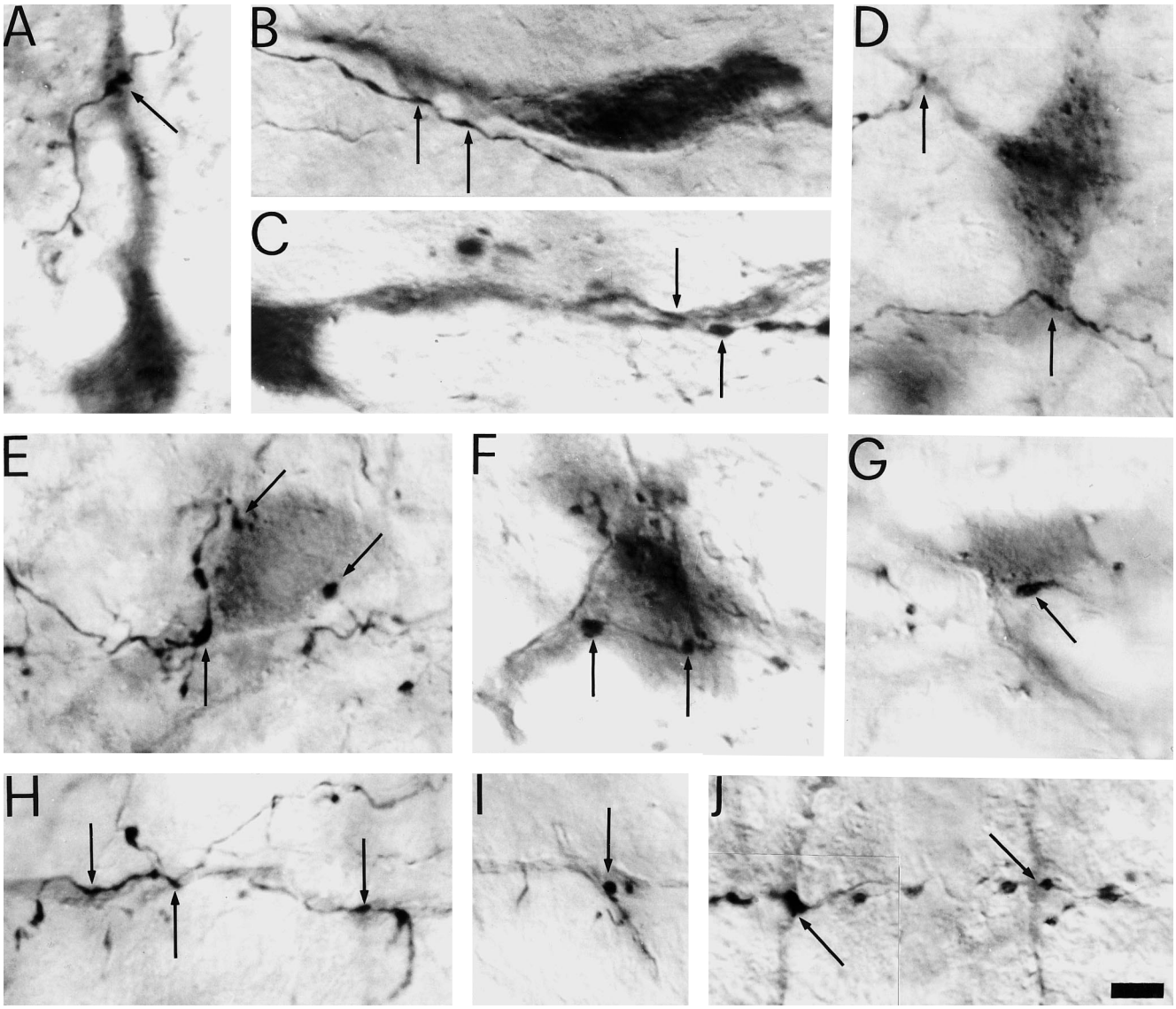

Fig. 6A–J. Dual-immunostained sections through the LPGi demonstrating PHA-L labeled auditory fibers from the CN co-distributed with 5-HT-ir profiles. **A–D** Black-stained beaded fibers and varicosities closely apposed to lighter stained 5-HT-ir primary dendritic processes. *Arrows* indicate presumed axo-dendritic synaptic contacts between auditory fibers and postsynatic targets. **E–G** Presumed axo-somatic synaptic contacts (*arrows*) between auditory fibers and 5-HT-ir somata. **H–J** Presumed axo-dendritic synaptic contacts (*arrows*) between auditory fibers and higher order 5-HT-ir dendritic processes. *Bar:* 10 μm for all panels

probably represented higher order dendrites (Fig. 6H–J). Varicosities juxtaposed to 5-HT-ir somata (Fig. 6E–G) were only rarely seen.

The co-distribution of CN fibers with PNMT-ir structures of C1 adrenergic neurons was only present in a small area in the LPGi where the posterior pole of the facial nucleus met the anterior pole of the rostroventrolateral reticular nucleus (Fig. 7). Accordingly, only the most rostral PNMT-ir neurons received potential synaptic contacts. Nevertheless, several contiguities between black-stained varicosities and brown-stained PNMT-ir elements could be verified, mainly on primary dendrites (Fig. 8A–D) and on higher order dendrites (Fig. 8E–H). In contrast, PNMT-ir somata appeared to be only occasionally contacted by labeled boutons (Fig. 8D).

Ultrastructural analysis

We analyzed labeled fibers from ultrathin sections with the electron microscope to investigate whether the large varicosities on identified auditory axons in the LPGi, as seen at the light-microscopic level, represented synapses. We found that labeled boutons exhibited the ultrastructural characteristics of functional synapses, such as obvious postsynaptic membrane thickenings, presynaptic vesicles, and organelles such as mitochondria (Fig. 9). The labeled boutons were found to make synaptic contacts predominantly with large dendritic shafts (e.g., Fig. 9D). The synapses had asymmetric postsynaptic densities (Gray type I) and round vesicles (Fig. 9C, D), indicative of excitatory synaptic transmission (Gray 1959). In a few cases, labeled and unlabeled boutons were found to terminate at the same dendritic shaft (Fig. 9C, E).

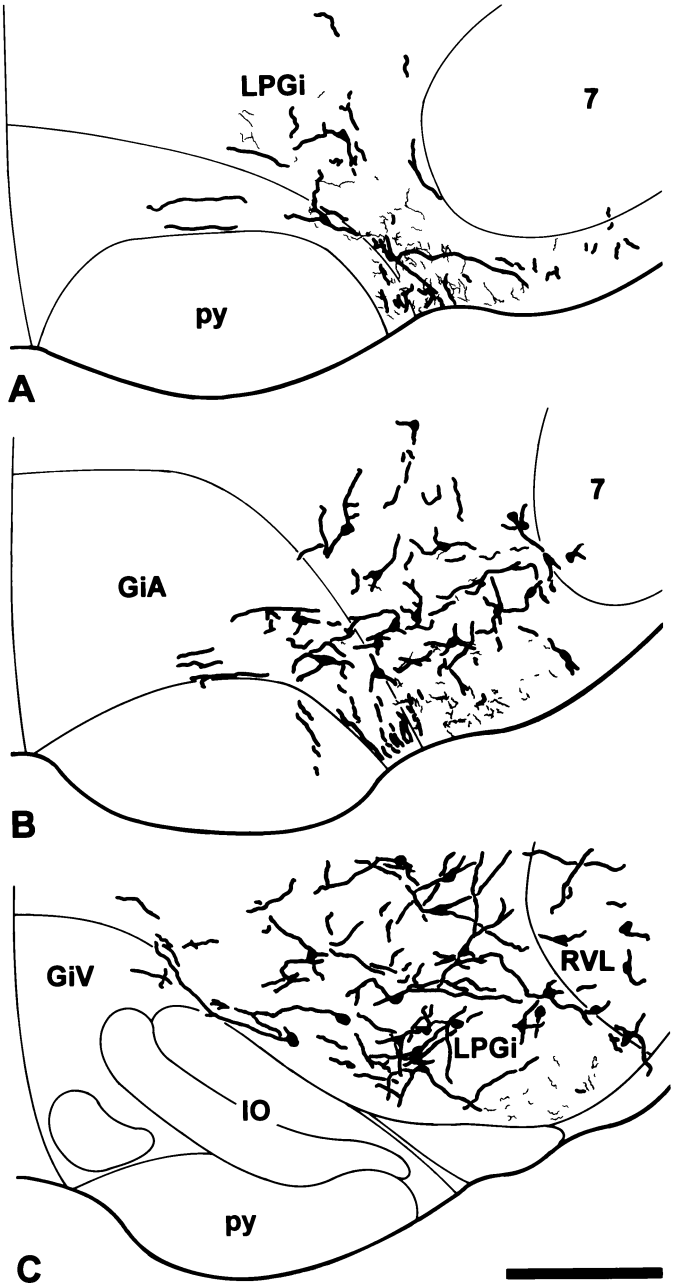

Fig. 7A–C. Camera lucida drawings of coronal sections through the medullary brainstem, from rostral to caudal, illustrating the co-distribution in the LPGi of anterogradely labeled auditory fibers from the CN (depicted by *thin curved lines*) and rostrally located PNMT-ir processes of neurons of the C1 adrenergic cell group (depicted by *thick lines*). *7* Facial nucleus; *GiA* gigantocellular reticular nucleus, alpha; *GiV* gigantocellular reticular nucleus, ventral; *IO* inferior olive; *py* pyramidal tract, *RVL* rostoventrolateral reticular nucleus. *Bar:* 500 μm

Discussion

In the present study, we have shown that the LPGi receives considerable auditory input that originates almost exclusively from neurons in the posteroventral CN and the cochlear root nucleus. Their axons terminate in the cell-poor ventral portion of the LPGi, which is however strongly invaded by beaded dendritic profiles. These dendrites belong mainly to parent cell bodies located in the dorsal half of the LPGi, as can be seen in the Golgi-stained material. Our double-labeling experiments have shown that the varicose auditory axons in the LPGi are often closely apposed to immunoreactive dendritic profiles of B3 serotonergic and Cl adrenergic neurons, indicating synaptic contacts of auditory terminal fibers with these transmitter-classified cells. Ultrastructural analysis has revealed that boutons found on labeled auditory axons do indeed form functional synapses; the latter are presumably excitatory in nature. Interestingly, these synapses are specifically associated with dendritic shafts of LPGi neurons, indicative of axo-dendritic contacts.

The LPGi of the rat, as defined in the present study, corresponds in location to the "juxtafacial portion of the nucleus paragigantocellularis" of Van Bockstaele et al. (1993), to the rostral half of the "nucleus paragigantocellularis lateralis" of Andrezik et al. (1981a), and to the rostral half of the "nucleus reticularis paragigantocellularis lateralis" of Newman (1985). With respect to the cytology of the LPGi, our observations are in general agreement with those of previous reports (Andrezik et al. 1981a; Newman 1985). In his Golgi study, Newman (1985) distinguishes four cell types based on their specific dendritic arborizations. The main cell type is characterized by several long, ventrally coursing dendrites that apparently extend into the spinoreticular fibers of the anterolateral system. These cells are also numerous in our material and their beaded dendrites seem to be the major targets of auditory axons, terminating ventrally in the LPGi. This assumption is strongly supported by our ultrastructural data, which have revealed almost exclusively axo-dendritic synapses in the LPGi.

Auditory projection to the LPGi

The observation that the LPGi receives input from auditory nuclei, including the CN and inferior colliculus, has been previously reported for the rat (Andrezik et al. 1981a, b; Kandler and Herbert 1991; Caicedo and Herbert 1993; Van Bockstaele et al. 1989, 1993) and cat (Errington and Dashwood 1979; Kamiya et al. 1988). In the present study, we have concentrated on the CN and demonstrate that the auditory afferents originate to a great extent from neurons in the posteroventral CN, in agreement with Andrezik's observations in the rat (Andrezik et al. 1981a, b), and from neurons located in the cochlear root nucleus. In contrast, the majority of LPGi-projecting neurons in the cat are found in the anteroventral CN (Kamiya et al. 1988).

Neurons in the rat posteroventral CN and the cochlear root nucleus have in common that they receive direct input from the spiral ganglion via the 8th nerve (Harrison and Irving 1966) and, thus, represent the first central relays for ascending auditory information. Neurons in the posteroventral CN receive input from all loci of the cochlea, as demonstrated by intracellular recordings (e.g., Friauf and Ostwald 1988) and by *c-fos* immunocytochemistry (Friauf 1992). Physiologically, neurons in the rat posteroventral CN have been characterized as "on"-

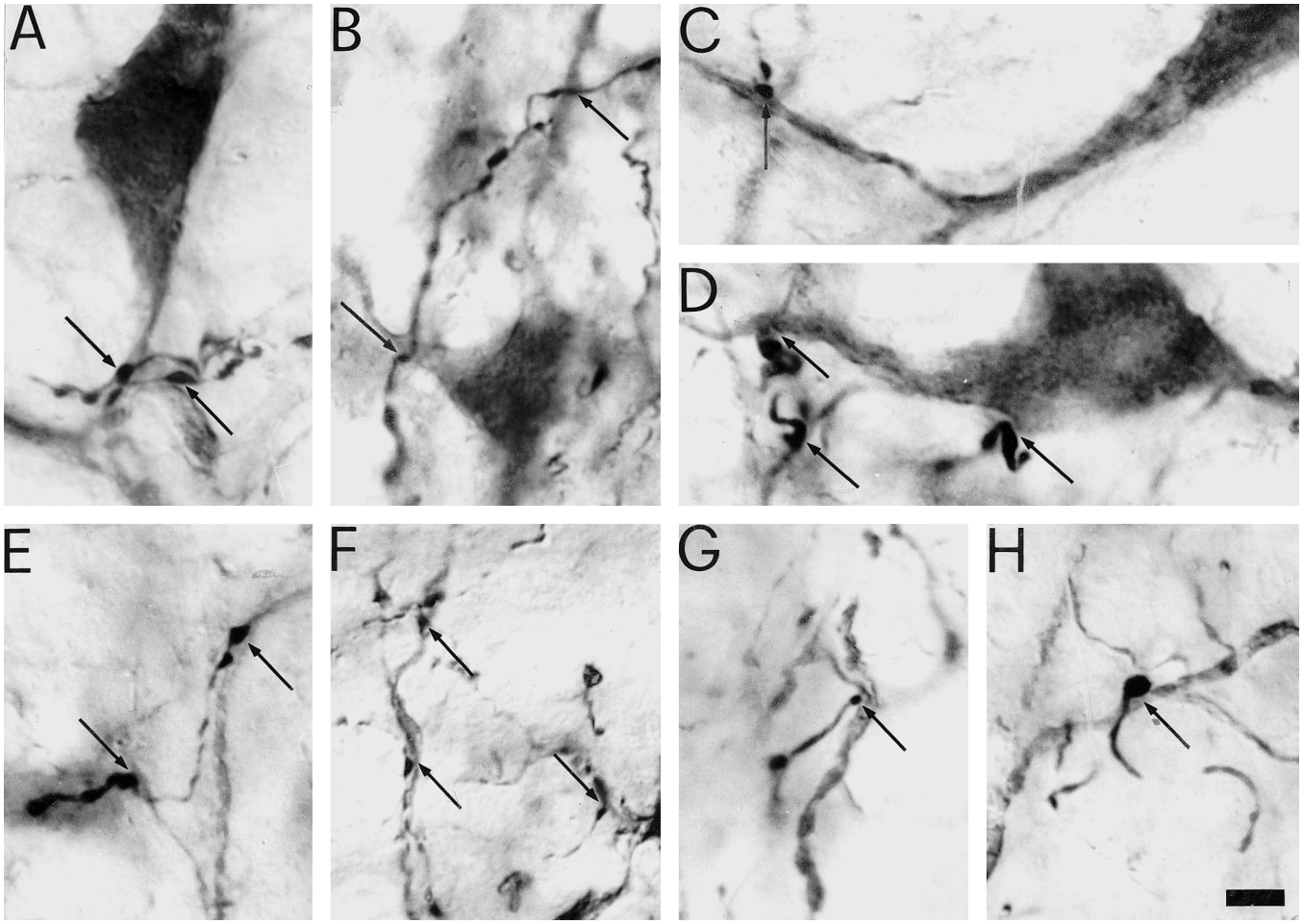

Fig. 8A–H. Dual-immunostained sections through the LPGi, demonstrating PHA-L labeled auditory fibers from the CN co-distributed with PNMT-ir structures. **A–D** Black-stained beaded fibers and varicosities closely apposed to lighter stained PNMT-ir primary dendritic processes and somata. *Arrows* indicate presumed axo-dendritic (**A–C**) or axo-somatic (**D**) synaptic contacts between auditory fibers and postsynaptic targets. **E–H** Presumed axo-dendritic synaptic contacts (*arrows*) between auditory fibers and higher order PNMT-ir dendritic profiles. *Bar:* 10 μm for all panels

cells or "primary like"-cells. The latter show response properties that are similar to those of auditory nerve fibers and largely preserve the temporal firing pattern of their input (for a review, see Oertel 1991).

The present study is the first to report that cochlear root neurons provide a major contribution to the auditory input in the LPGi. The cochlear root nucleus (corresponding to the "acoustic nerve nucleus"; Harrison et al. 1962; Harrison and Irving 1966) consists of large multipolar cells that are embedded in the anterolateral portion of the acoustic nerve. Their dendrites run perpendicular or parallel to the ascending axons of the 8th nerve, the latter providing the major input to the cochlear root neurons (Merchan et al. 1988; López et al. 1993). Furthermore, tracing experiments indicate that the terminating axons originate primarily from the base of the cochlea, i.e., from the high frequency segment (Osen et al. 1991). Cochlear root neurons give rise to large diameter axons that enter the brainstem via the trapezoid body (Merchan et al. 1988). As yet, little is known about their specific targets. López et al. (1993) have reported projections of rat cochlear root neurons to the paralemniscal region and to the deep layers of the superior colliculus. Previous studies in our laboratory have shown that cochlear root neurons also project to other extra-auditory areas, including the ventrolateral tegmental area (Klepper and Herbert 1993) and the caudal pontine reticular nucleus, where they probably serve audio-motor functions (Lingenhöhl and Friauf 1994). From these data, the cochlear root neurons seem to project exclusively to extra-auditory targets and thus, do not play a role in processing acoustic signals along the auditory pathway. This makes them unique compared with all other neurons of the CN. The finding that cochlear root neurons contain neither γ-aminobutyric-acid-like nor glycine-like immunoreactivity (Osen et al. 1991) strongly suggests that they transmit acoustic information by means of excitatory neurotransmission. This is in agreement with our data derived from the electron-microscopic material, viz., that auditory synapses observed in the LPGi have asymmetric postsynaptic densities and round vesicles and thus probably represent Gray type I excitatory synapses (Gray 1959).

To summarize, anatomical and physiological data demonstrate that neurons of the posteroventral CN and

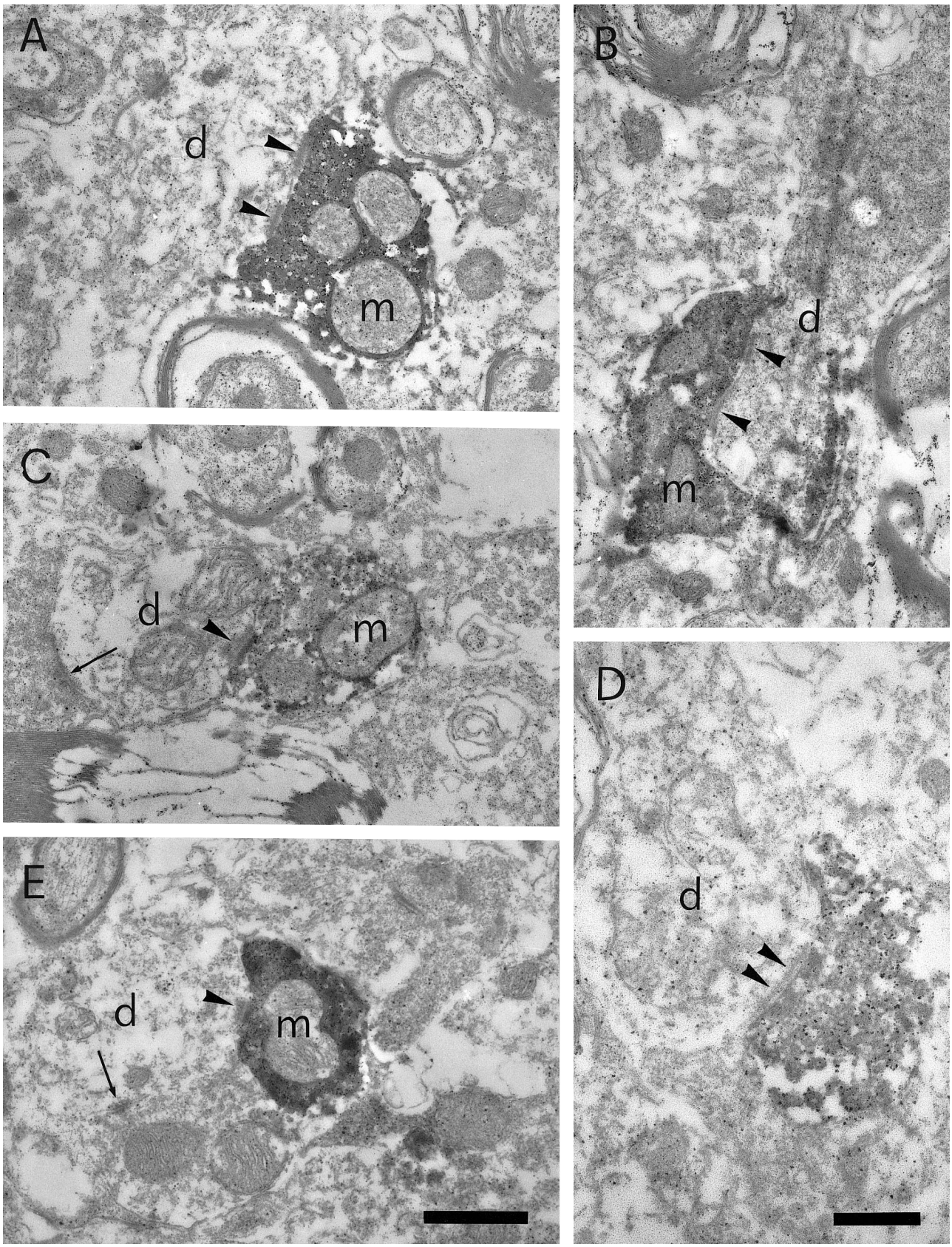

Fig. 9A–E. Examples of labeled presynaptic boutons that form asymmetric, presumably excitatory synapses (*arrowheads*) with postsynaptic dendritic shafts (*d*) in the LPGi. Unlabeled asymmetric synapes are also found at the same dendritic shafts (*arrow* in **C** and **E**). Note the perforation in the postsynaptic density (seen between *arrowheads* in **A**). In most labeled boutons, mitochondria (*m*) can be readily recognized. Round vesicles can also be seen in the labeled boutons shown in **C** and **D**. Bar: in **E** 1 μm (also for **A–C**); in **D** 0.5 μm

the cochlear root nucleus receive acoustic information that comes directly from the cochlea and that is then monosynaptically relayed to the LPGi. It has been proposed that cochlear root neurons are the first central neurons to receive acoustic information and that they are probably driven by loud, high frequency sounds (for a review, see López et al. 1993). Moreover, because of their thick, fast conducting axons, cochlear root neurons are ideal candidates for transmitting the occurrence of loud acoustic signals most rapidly to extra-auditory areas along the neuraxis. The auditory information of neurons in the posteroventral CN is still "primary-like" or just codes for the "onset" of an acoustic event. Furthermore, the LPGi projecting neurons of the posteroventral CN seem to receive the complete frequency spectrum of the cochlea, and their axons may converge within one locus in the LPGi. This suggests that the major function of the pathway lies in the fast transmission of acoustic events in general to an extra-auditory reticular area.

Postsynaptic targets

A major aim of the present study has been to identify potential targets of auditory axons in the LPGi. Neurons can be easily classified in terms of their neurotransmitter or their transmitter-synthesizing enzyme. By means of specific antisera, not only can the somata be stained, but also the proximal and distal dendrites. The latter represent the main target profiles of efferent axons. Thus, double-labeling experiments should provide light-microscopic evidence as to whether specific transmitter-ir profiles are contacted by auditory axons.

Serotonergic neurons In the present study, we have shown that auditory axons are most often found closely apposed to serotonergic (5-HT-ir) neurons located within the LPGi; these neurons constitute the lateral portion of the B3 cell group (e.g., Steinbusch 1981). They have widespread projections within the pons and the medulla, sending fibers especially to autonomic and respiratory cell groups in the nucleus of the solitary tract, to the ventrolateral medulla, and to the cranial motor nuclei (for a recent review, see Halliday et al. 1995). Prominent projections of these laterally located B3 neurons to the spinal cord have also been reported (Millhorn et al. 1989; Bowker and Abbott 1990; Jones et al. 1991; Jones and Light 1992). In the spinal cord, serotonergic terminal fibers are present in the superficial layers of the dorsal horn (Marlier et al. 1991; Kwiat and Basbaum 1992), suggesting that this input plays a role in the processing of afferent somatosensory information, such as the supression of nociceptive inputs (for a review, see Fields et al. 1991). Indeed, load acoustic stimuli can produce analgesia (Cranney 1988). However, whether the pathway demonstrated in the present study plays a role for mediating this effect remains to be elucidated. A most dense 5-HT-ir plexus is found amongst neurons of the intermediolateral and intermediomedial cell column (Anderson et al. 1989; Newton and Hamill 1989) where they synapse on preganglionic sympathic neurons (Poulat et al. 1992). Since serotonergic B3 neurons contribute to this innervation (Loewy and McKellar 1981; Sasek et al. 1990; Allen and Cechetto 1994), it is conceivable that they influence the sympathetic outflow. Moreover, serotonergic projections to spinal motoneurons have been reported (e.g., Ozaki et al. 192; Allen and Cechetto 1994). Thus, B3 serotonergic neurons of the LPGi are probably involved in diverse systems that control a variety of different functions.

Adrenergic neurons Our double-stained material provides compelling evidence that varicose auditory fibers form putative synaptic contacts with PNMT-ir somata and dendrites in the rostral aspect of the Cl adrenergic cell group. This cell group has been the focus of numerous anatomical and physiological studies that link the Cl cells almost exclusively with autonomic functions. The majority of the Cl adrenergic neurons send projections to spinal cord autonomic cells (Ross et al. 1984a; Tucker et al. 1987; Sawchenko and Bohn 1989; Minson et al. 1990; Mtui et al. 1995) where they form functional synapses with preganglionic sympathetic neurons (Milner et al. 1988; Bernstein-Goral and Bohn 1989). This pathway has been implicated in the control of sympathetic outflow and in particular with the regulation of vasomotor tone (Ross et al. 1984b; Morrison et al. 1988; Haselton and Guyenet 1989). Cl neurons also project to the nucleus of the solitary tract and to the dorsal motor nucleus of the vagus (Mtui et al. 1995) where they participate in baroreceptor reflex responses (Granata et al. 1985) and in the modulation of vagal outflow, respectively. Furthermore, Cl projections to the locus coeruleus (Guyenet and Young 1987; Pieribone et al. 1988; Pieribone and Aston-Jones 1991), to the periaqueductal gray (Herbert and Saper 1992), to the amygdaloid complex (Roder and Ciriello 1993), and to hypothalamic nuclei (Tucker et al. 1987; Sawchenko and Bohn 1989; Cunningham et al. 1990; Phillipson and Bohn 1994) may control and coordinate specific autonomic, endocrine, and behavioral functions.

In conclusion, our anatomical data provide the first evidence for a monosynaptic auditory input from the cochlear nuclear complex to B3 serotonergic and Cl adrenergic neurons in the LPGi. This pathway enables acoustic events to be rapidly transmitted to an extra-auditory reticular area. Primary auditory input may modulate the activity of B3 serotonergic and Cl adrenergic cells and thus might participate in the induction of adaptive behavior or changes of autonomic and limbic functions in response to acoustic stimuli.

Acknowledgements. The authors thank Dr. Heinz Schwarz (MPI for Developmental Biology) for his valuable help with the electron-microscopic techniques, Helga Zillus for expert technical assistance, and Doris Fink for correcting the English.

References

Allen GV, Cechetto DF (1994) Serotonergic and nonserotoninergic neurons in the medullary raphe system have axon collateral projections to autonomic and somatic cell groups in the medulla and spinal cord. J Comp Neurol 350:357–366

Anderson CR, McLachlan EM, Christhie OSRB (1989) Distribution of sympathetic preganglionic neurons and monoaminergic nerve terminals in the spinal cord of the rat. J Comp Neurol 283:269–284

Andrezik JA, Chan-Palay V, Palay SL (1981a) The nucleus paragigantocellularis lateralis in the rat. Conformation and cytology. Anat Embryol 161:355–371

Andrezik JA, Chan-Palay V, Palay SL (1981b) The nucleus paragigantocellularis lateralis in the rat. Demonstration of afferents by the retrograde transport of horseradish peroxidase. Anat Embryol 161:373–390

Aston-Jones G, Ennis M, Pieribone VA, Nickell WT, Shipley MT (1986) The brain nucleus locus coeruleus: restricted afferent control of a broad efferent network. Science 234:734–740

Bellintani-Guardia B, Caicedo A, Kandler K, Naskar R, Herbert H (1994) Auditory projections to the lateral paragigantocellular nucleus in the rat: a potential site for sensory-autonomic integration? In: Elsner N, Breer H (eds) Proceedings of the 22nd Göttingen Neurobiology Conference. Stuttgart, pp 614

Bernstein-Goral H, Bohn C (1989) Phenylethanolamine N-methyltransferase immunoreactive terminals synapse on adrenal preganglionic neurons in the rat spinal cord. Neuroscience 32:521–537

Bowker RM, Abbott LC (1990) Quantitative re-evaluation of descending serotonergic projections from the medulla of the rodent: evidence for existence co-existence of serotonin and peptides in the same spinally projecting neurons, but not from the nucleus raphe magnus. Brain Res 512:15–25

Caicedo A, Herbert H (1993) Topography of descending projections from the inferior colliculus to auditory brainstem nuclei in the rat. J Comp Neurol 328:377–392

Cranney J (1988) Analgesia following startle-eliciting stimuli. Psychobiology 16:67–69

Cunningham ET, Bon MC, Sawchenko PE (1990) Organization of adrenergic inputs to the paraventricular and supraoptic nuclei of the hypothalamus in the rat. J Comp Neurol 292:651–667

Dobbins EG, Feldman JL (1994) Brainstem network controlling descending drive to phrenic motoneurons in rat. J Comp Neurol 347:64–86

Eldred W, Zucker C, Karten HJ, Yazulla S (1983) Comparison of fixation and penetration enhancement techniques for use in ultrastructural immunocytochemistry. J Histochem Cytochem 31:285–292

Errington ML, Dashwood MR (1979) Projections to the ventral surface of the cat brainstem demonstrated by horseradish peroxidase. Neurosci Lett 12:153–158

Fields HL, Heinricher MM, Mason P (1991) Neurotransmitters in nociceptive modulatory circuits. Annu Rev Neurosci 14:219–245

Friauf E (1992) Tonotopic order in the adult and developing auditory system of the rat as shown by c-fos immunocytochemistry. Europ J Neurosci 4:798–812

Friauf E, Ostwald J (1988) Divergent projections of physiologically characterized rat ventral cochlear nucleus neurons as shown by intra-axonal injection of horseradish peroxidase. Exp Brain Res 73:263–284

Granata AR, Ruggiero DA, Park DH, Joh TH, Reis DJ (1985) Brain stem area with Cl epinephrine neurons mediates baroreflex vasodepressor responses. Am J Physiol 248:H547–H567

Gray EG (1959) Electron microscopy of synaptic contacts on dendritic spines of the cerebral cortex. Nature 183:1592–1593

Guyenet PG, Young BS (1987) Projections of nucleus paragigantocellularis lateralis to locus coeruleus and other structures in the rat. Brain res 406:171–184

Halliday G, Harding A, Paxinos G (1995) Serotonin and tachykinin systems. In: Paxinos G (ed) The rat nervous system. Academic Press, Sydney, pp 929–974

Harrison JM, Irving R (1966) The organization of the posterior ventral cochlear nucleus in the rat. J Comp Neurol 126:392–402

Harrison JM, Warr WB, Irving RE (1962) Second order neurons in the acoustic nerve. Science 138:893–895

Haselton JR, Guyenet PG (1989) Electrophysiological characterization of putative Cl adrenergic neurons in the rat. Neuroscience 30:199–214

Haxhiu MA, Jansen ASP, Cherniack NS, Loewy AD (1993) CNS innervation of airway-related parasympathetic preganglionic neurons: a transneuronal labeling study using pseudorabies virus. Brain Res 618:115–134

Herbert H (1992) Evidence for projections from the medullary nuclei onto serotonergic and dopaminergic neurons in the midbrain dorsal raphe nucleus of the rat. Cell Tissue Res 270:149–156

Herbert H, Saper CB (1992) Organization of medullary adrenergic and noradrenergic projections to the periaqueductal gray matter in the rat. J Comp Neurol 315:34–52

Jones BE, Holmes CJ, Rodriguez-Veiga E, Mainville L (1991) GABA-synthesizing neurons in the medulla: their relationship to serotonin-containing and spinally projecting neurons in the rat. J Comp Neurol 313:349–367

Jones SL, Light AR (1992) Serotonergic medullary raphespinal projection to the lumbar spinal cord in the rat: a retrograde immunohistochemical study. J Comp Neurol 322:599–610

Joseph SA, Piekut DT (1986) Dual immunostaining procedure demonstrating neurotransmitter and neuropeptide codistribution in the same brain section. Am J Anat 175:331–342

Kandler K, Herbert H (1991) Auditory projections from the cochlear nucleus to pontine and mesencephalic reticular nuclei in the rat. Brain Res 562:230–242

Kamiya H, Itoh K, Yasui Y, Ino T, Mizuno N (1988) Somatosensory and auditory relay nucleus in the rostral part of the ventrolateral medulla: a morphological study in the cat. J Comp Neurol 273:421–435

Klepper A, Herbert H (1993) The ventrolateral tegmental nucleus in the rat: analysis of the afferent and efferent connections. Soc Neurosci Abstr 19:989

Kwiat GC, Basbaum AI (1992) The origin of brainstem noradrenergic and serotonergic projections to the spinal cord dorsal horn in the rat. Somatosens Mot Res 2:157–173

Lingenhöhl K, Friauf E (1992) Giant neurons in the caudal pontine reticular formation receive short latency acoustic input: an intracellular recording and HRP-study in the rat. J Comp Neurol 325:473–492

Lingenhöhl K, Friauf E (1994) Giant neurons in the rat reticular formation: a sensorimotor interface in the elementary acoustic startle circuit? J Neurosci 14:1176–1194

Loewy AD, McKellar S (1981) Serotonergic projections from the ventral medulla to the intermediolateral cell column in the rat. Brain Res 211:146–152

Loewy AD, Wallach JH, McKellar S (1981) Efferent connections of the ventral medulla oblongata in the rat. Brain Res Rev 3:63–80

López DE, Merchán MA, Bajo VM, Saldaña E (1993) The cochlear root neurons in the rat, mouse and gerbil. In: Merchán MA, Juiz JM, Godfrey DA (eds) The mammalian cochlear nuclei: organization and function. Plenum, New York, pp 291–301

Marlier L, Sandillon F, Poulat P, Rajaofetra N, Geffard M, Privat A (1991) Serotonergic innervation of the dorsal horn of the rat spinal cord: light and electron microscopic immunocytochemical study. J Neurocytol 20:310–322

Merchán MA, Collia F, López DE, Saldaña E (1988) Morphology of cochlear root neurons in the rat. J Neurocytol 17:711–725

Millhorn DE, Hökfelt T, Verhofstad AAJ, Terenius L (1989) Individual cells in the raphe nuclei of the medulla oblongata in rat that contain immunoreactivities for both serotonin and enkephalin project to the spinal cord. Exp Brain Res 75:536–542

Milner TA, Morrison SF, Abate C, Reis DJ (1988) Phenylethanolamine-N-methyltransferase-containing terminals synapse directly on sympathetic preganglionic neurons in the rat. Brain Res 448:205–222

Minson J, Llewellyn-Smith I, Nevilla A, Somogyi P, Chalmers J (1990) Quantitative analysis of spinally projecting adrenaline-synthesising neurons of C1, C2 and C3 groups in rat medulla oblongata. J Auton Nerv Syst 30:209–220

Morrison SF, Milner TA, Reis DJ (1988) Reticulospinal vasomotor neurons of the rat rostral ventrolateral medulla: relationship to sympathetic nerve activity and the C1 adrenergic cell group. J Neurosci 8:1286–1301

Mtui EP, Anwar M, Reis DJ, Ruggiero DA (1995) Medullary visceral reflex circuits: local afferents to nucleus tractus solitarii synthesize catecholamines and project to thoracic spinal cord. J Comp Neurol 351:5–26

Newman DB (1985) Distinguishing rat brainstem reticulospinal nuclei by their neuronal morphology. I. Medullary nuclei. J Hirnforsch 26:187–226

Newton BW, Hamill RW (1989) Immunohistochemical distribution of serotonin in spinal autonomic nuclei. I. Fiber patterns in the adult rat. J Comp Neurol 279:68–81

Oertel D (1991) The role of intrinsic neuronal properties in the encoding of auditory information in the cochlear nuclei. Curr Opin Neurobiol 1:221–228

Osen KK, Lopez DE, Slyngstad TA, Ottersen OP, Storm-Mathisen J (1991) GABA-like and glycine-like immunoreactivities of the cochlear root nucleus in rat. J Neurocytol 20:17–25

Ozaki S, Kudo N, Okado N (1992) Immunohistochemical study on development of serotonin-, substance P-, and enkephalin-positive fibers in the rat spinal motor nucleus. J Comp Neurol 325:462–470

Paxinos G, Watson C (1986) The rat brain in stereotaxic coordinates. Academic Press, Sydney

Phillipson OT, Bohn MC (1994) C1–3 adrenergic medullary neurones project to the paraventricular thalamic nucleus in the rat. Neurosci Lett 176:67–70

Pieribone VA, Aston-Jones G (1991) Adrenergic innervation of the rat nucleus locus coeruleus arises predominantly from C1 adrenergic cell group in the rostral medulla. Neuroscience 41:525–542

Pieribone VA, Aston-Jones G, Bohn MC (1988) Adrenergic and non-adrenergic neurons in the C1 and C3 areas project to locus coeruleus: a fluorescent double labeling study. Neurosci Lett 85:297–303

Poulat P, Marlier L, Rajaofetra N, Privat A (1992) 5-Hydroxytryptamine, substance P and thyrotropin-releasing hormone synapses in the intermediolateral cell column of the rat thoracic spinal cord. Neurosci Lett 136:19–22

Roder S, Ciriello J (1993) Innervation of the amygdaloid complex by catecholaminergic cell groups of the ventrolateral medulla. J Comp Neurol 332:105–122

Ross CA, Ruggiero DA, Joh TH, Park DH, Reis DJ (1984a) Rostral ventrolateral medulla: selective projections to the thoracic autonomic cell column from the region containing C1 adrenaline neurons. J Comp Neurol 228:168–185

Ross CA, Ruggiero DA, Park DH, Joh TH, Sved AF, Fernandez-Pardal J, Saavedra JM, Reis DJ (1984b) Tonic vasomotor control by the rostral ventrolateral medulla: effect of electrical or chemical stimulation of the area containing C1 adrenaline neurons on arterial pressure, heart rate, and plasma catecholamines and vasopressin. J Neurosci 2:474–494

Sasek CA, Wessendorf MW, Helke CJ (1990) Evidence for co-existence of thyrotropin-releasing hormone, substance P and serotonin in ventral medullary neurons that project to the intermediolateral cell column in the rat. Neuroscience 35:105–119

Sawchenko PE, Bohn MC (1989) Glucocorticoid receptor-immunoreactivity in C1, C2 and C3 adrenergic neurons that project to the hypothalamus or to the spinal cord in the rat. J Comp Neurol 285:107–116

Steinbusch HWM (1981) Distribution of serotonin-immunoreactivity in the central nervous system of the rat – cell bodies and terminals. Neuroscience 6:557–618

Strack AM, Sawyer WB, Platt KB, Loewy AD (1989) CNS cell groups regulating the sympathetic outflow to adrenal gland as revealed by transneuronal cell body labeling with pseudorabies virus. Brain Res 491:274–296

Tucker DC, Saper CB, Ruggiero DA, Reis DJ (1987) Organization of central adrenergic pathways. I. Relationships of ventrolateral medullary projections to the hypothalamus and spinal cord. J Comp Neurol 259:591–603

Von Bockstaele EJ, Akaoka H, Aston-Jones G (1993) Brainstem afferents to the rostral (juxtafacial) nucleus paragigantocellularis: integration of the exteroceptive and interoceptive sensory inputs in the ventral tegmentum. Brain Res 603:1–18

Van Bockstaele EJ, Pieribone VA, Aston-Jones G (1989) Diverse afferents converge on the nucleus paragigantocellularis in the rat ventrolateral medulla: retrograde and anterograde tracing studies. J Comp Neurol 290:561–584

Zagon A, Smith AD (1993) Monosynaptic projections from the rostral ventrolateral medulla oblongata to identified sympathetic preganglionic neurons. Neuroscience 54:729–743

Zagon A, Totterdell S, Jones RSG (1994) Direct projections from the ventrolateral medulla oblongata to the limbic forebrain: anterograde and retrograde tract-tracing studies in the rat. J Comp Neurol 340:445–468